

## Electronic Supporting Information

# Water Adsorption, Dissociation and Oxidation on SrTiO<sub>3</sub> and Ferroelectric Surfaces Revealed by Ambient Pressure X-ray Photoelectron Spectroscopy

Neus Domingo,<sup>†\*</sup> Elzbieta Pach,<sup>†</sup> Kumara Cordero-Edwards,<sup>†</sup> Virginia Pérez-Dieste,<sup>‡</sup> Carlos Escudero,<sup>‡</sup> Albert Verdaguer<sup>§\*</sup>

<sup>†</sup> Catalan Institute of Nanoscience and Nanotechnology (ICN2), CSIC and The Barcelona Institute of Science and Technology, Campus UAB, Bellaterra, 08193 Barcelona, Spain

<sup>‡</sup>ALBA Synchrotron Light Source, Carrer de la Llum 2–26, 08290 Cerdanyola del Vallès, Barcelona, Spain

<sup>§</sup>Institut de Ciència de Materials de Barcelona ICMAB-CSIC, Campus de la UAB, E-08193 Bellaterra, Spain

## A. FERROELECTRIC CHARACTERIZATION:

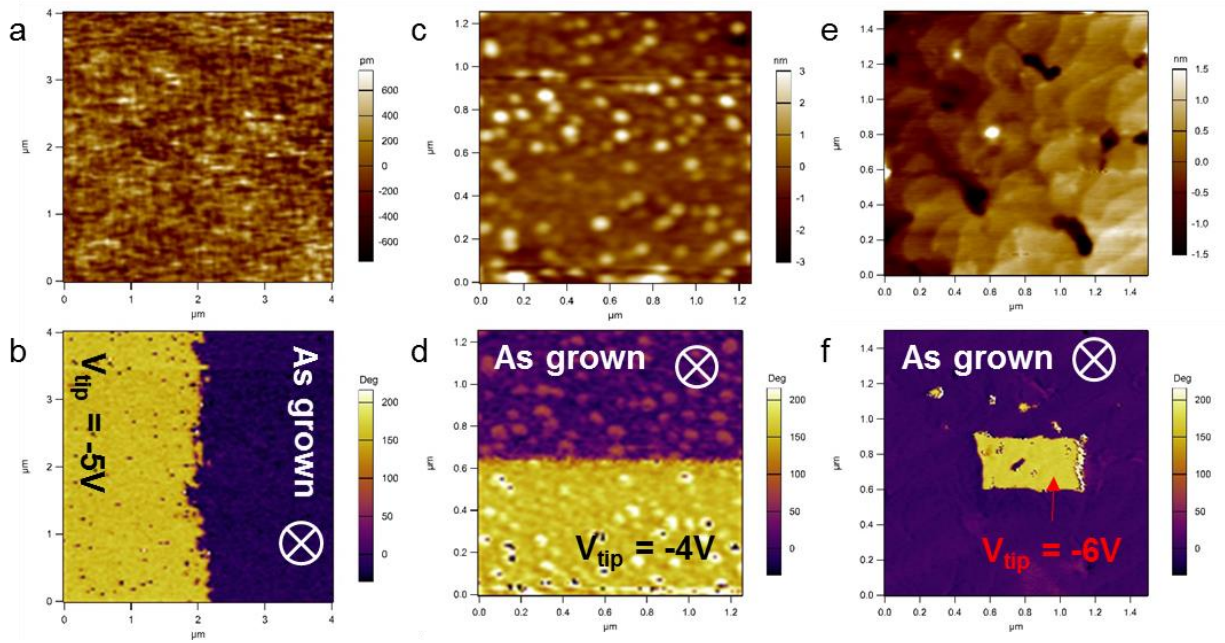


**Fig. S1:** Ferroelectric characterization of thin films with Piezoresponse Force Microscopy. In order to probe the as grown ferroelectric polarization direction of the thin films, selected areas were scanned by applying a  $V_{tip} > 0$  to probe ferroelectric polarization switching from down to up state. Top images are the topographies of ferroelectric thin films for a) PZT, c) BTO and e) BFO. Bottom images correspond to the out of plane PFM phase images for b) PZT, d) BTO and f) BFO, where purple corresponds to polarization direction pointing inwards and yellow areas determine polarization pointing out of the surface plane. It is to mention that BFO (001) thin films also contain some in-plane polarization component, since BFO has a rhombohedral structure in the FE phase and the polarization points to the vertices of the unit cell.

## Cleaning of the sample:

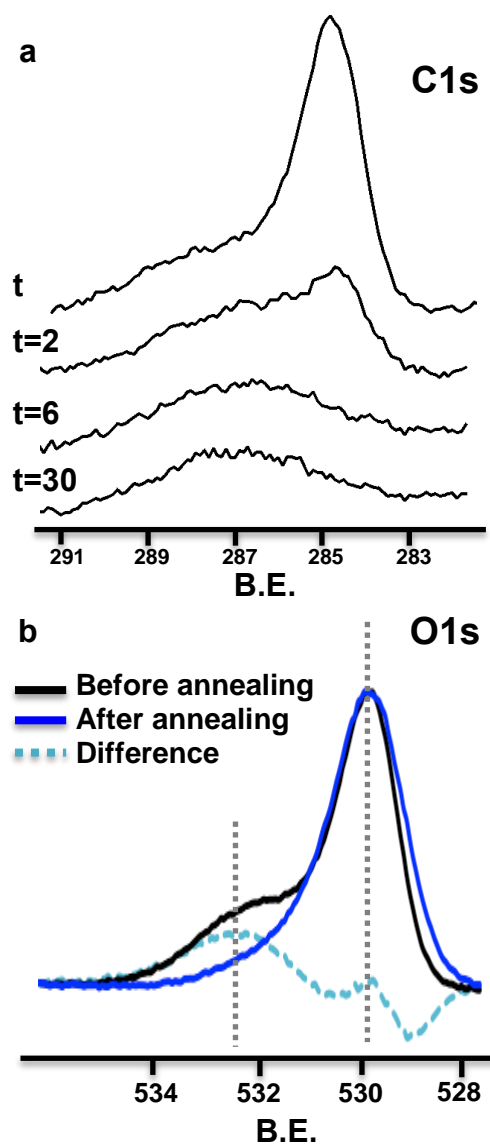


**Fig. S2:** a) XPS C1s spectra of the SrTiO<sub>2</sub>(001) surface as it exposed to 0.1 mbar of O<sub>2</sub> and annealed at 200 °C. Initial spectrum (t=0) corresponds to the spectrum measured before O<sub>2</sub> was introduced in the chamber. For times larger than a few minutes the spectra remain unchanged. b) XPS O1s spectra after and before annealed at 200°C with O<sub>2</sub>. The difference between the two spectra is shown, revealing the position of the main peak related to carbon species (~1.8 eV from the bulk oxide peak) that have been removed during the annealing procedure.

## B. Fittings of O1s spectra:

### B1. Fitting parameters

The intensity of the O1s photoemission spectra was decomposed after subtracting a Shirley-type background. The relative ratio of Gaussian to Lorentzian line shape was chosen to visually best match the spectral shape observed experimentally: 30% Lorentzian was used for all spectra except for gas phase peak where a 70% Lorentzian was needed. The fitting parameters are shown in table S1 below. FWHM and BE indicates the range of energies for the different fittings, not the constrains used for the fitting procedure. The fitting constrains are already mentioned in the manuscript.

		Oxide(bulk)	Hydroxyls	COx	Surface-O	Water	Water(gas)
SrTiO <sub>3</sub>	% Lorentzian	30	30	30	30	30	70
	FWHM (eV)	0.9-1.1	1.3-1.4	1.1-1.3	1.3-1.5	1.4-1.6	0.4-0.6
	BE (eV)	529.8-529.9	530.7-531	531.6-531.8	532.3-532.6	533,4-533.7	535.5-535.7
BaTiO <sub>3</sub>	% Lorentzian	30	30	30	30	30	70
	FWHM (eV)	0.9-1.2	1.3-1.5	1.3-1.5	1.5-1.6	1.4-1.7	0.6-0.8
	BE (eV)	529.1-529.3	530.2-530.3	531-531.4	531.8-532	532.9-533.2	535.3-535.4
PbTi <sub>0.8</sub> Zr <sub>0.2</sub> O <sub>3</sub>	% Lorentzian	30	30	30	30	30	70
	FWHM (eV)	1-1.1	1.4-1.5	1.4-1.6	1.4-1.5	1.4-1.5	0.4-0.6
	BE (eV)	530.2-530.3	531.1-531.3	532-532.3	533-533.3	534.1-534.3	535.3-535.5
BiFeO <sub>3</sub>	% Lorentzian	30	30	30	30	30	70
	FWHM (eV)	1-1.1	1.4-1.5	1.1-1.3	1.4-1.5	1.4-1.5	0.4-0.5
	BE (eV)	529.6-529.8	530.5-530.7	531.4-531.6	532.2-532.5	533.3-533.5	535.3-535.4

**Table S1:** Fitting parameters for the O1s spectra.

## B2. Fitting of O1s Spectra at different pressure and temperature conditions

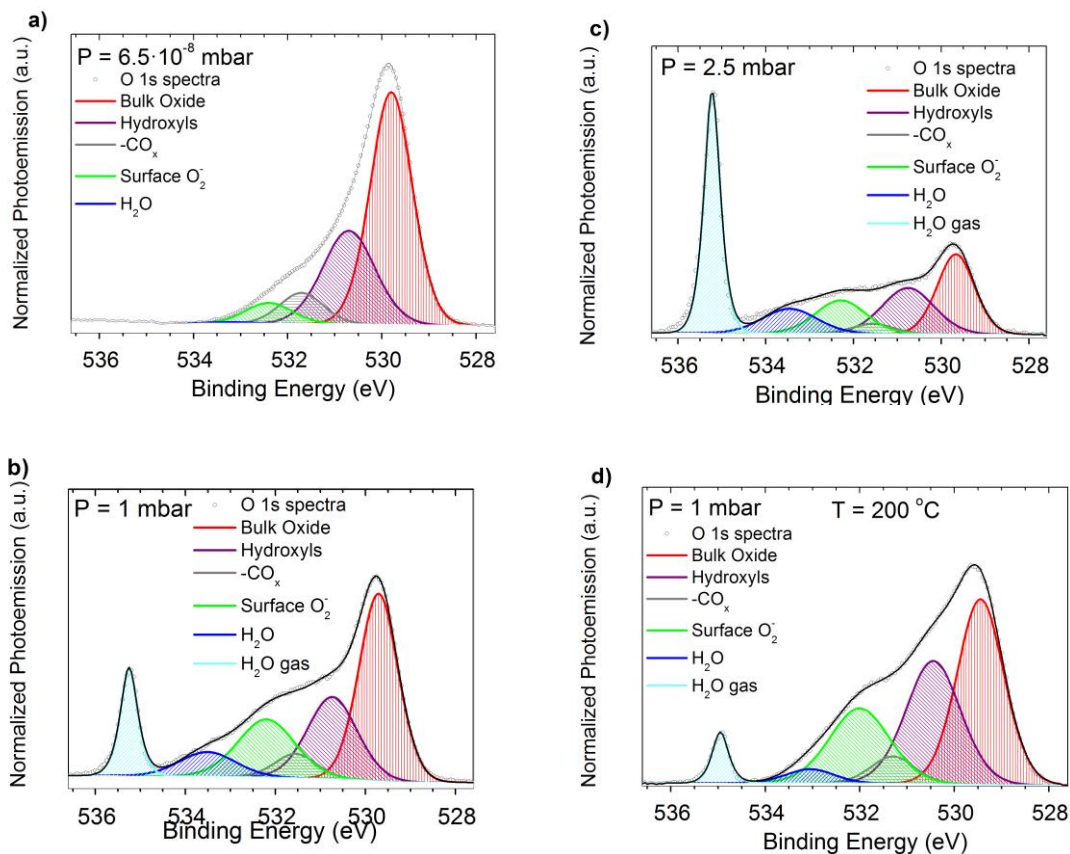


**Fig S3:** Decomposition of XPS spectra of O1s regions shown in Figure 1a, into the described peaks, for three different pressures at room temperature a)  $6.5 \cdot 10^{-8}$  mbar, b) 1 mbar and c) 2.5 mbar. The results of the fittings for each species as a function of pressure are shown in Figure 3a. d) The corresponding fitting at 1 mbar and 200 °C, with the results shown in Figure 3b.

### B3. Multilayer electron attenuation model for coverage calculations.

The model considers each species as a continuum slab in a multilayer configuration, characterized by its oxygen atomic density ( $N$ ), photoionization cross-section ( $\sigma$ ), thickness ( $t$ ) and inelastic mean free path ( $\lambda$ ).

The XPS intensities ( $I$ ) of all components in the model were expressed as:

$$I_{H_2O} \sim N_{H_2O} \sigma_{H_2O} \lambda_{H_2O} \left[ 1 - \exp\left(-\frac{t_{H_2O}}{\lambda_{H_2O}}\right) \right] \quad (1)$$

$$I_{SurfO} \sim N_{SurfO} \sigma_{SurfO} \lambda_{SurfO} \exp\left(-\frac{t_{H_2O}}{\lambda_{H_2O}}\right) \left[ 1 - \exp\left(-\frac{t_{SurfO}}{\lambda_{SurfO}}\right) \right] \quad (2)$$

$$I_{CO_x} \sim N_{CO_x} \sigma_{CO_x} \lambda_{CO_x} \exp\left(-\frac{t_{H_2O}}{\lambda_{H_2O}}\right) \left[ 1 - \exp\left(-\frac{t_{CO_x}}{\lambda_{CO_x}}\right) \right] \quad (3)$$

$$I_{OH} \sim N_{OH} \sigma_{OH} \lambda_{OH} \exp\left(-\frac{t_{H_2O}}{\lambda_{H_2O}}\right) \exp\left(-\frac{t_{SurfO}}{\lambda_{SurfO}}\right) \exp\left(-\frac{t_{CO_x}}{\lambda_{CO_x}}\right) \left[ 1 - \exp\left(-\frac{t_{OH}}{\lambda_{OH}}\right) \right] \quad (4)$$

$$I_{Ox} \sim N_{Ox} \sigma_{Ox} \lambda_{Ox} \exp\left(-\frac{t_{H_2O}}{\lambda_{H_2O}}\right) \exp\left(-\frac{t_{SurfO}}{\lambda_{SurfO}}\right) \exp\left(-\frac{t_{CO_x}}{\lambda_{CO_x}}\right) \exp\left(-\frac{t_{OH}}{\lambda_{OH}}\right) \quad (5)$$

where  $\sigma$  is assumed to have minor variations for the different species, i.e.  $\sigma_{Ox} \sim \sigma_{OH} \sim \sigma_{CO_x} \sim \sigma_{SurfO} \sim \sigma_{H_2O}$ . SurfO and CO<sub>x</sub> are considered as two different layers at the same distance from the surface.

By taking the intensity ratios, the thicknesses ( $t_{OH}$ ,  $t_{CO_x}$ ,  $t_{SurfO}$ ,  $t_{H_2O}$ ) of the different species can be determined:

$$t_{OH} = \lambda_{OH} \ln(1 + R_{Ox}^{OH}) \quad (6)$$

$$t_{SurfO} = \lambda_{SurfO} \ln\left(1 + \frac{R_{Ox}^{SurfO}}{\exp\left(-\frac{t_{OH}}{\lambda_{OH}}\right) \exp\left(-\frac{t_{CO_x}}{\lambda_{CO_x}}\right)}\right) \quad (7)$$

$$t_{CO_x} = \lambda_{CO_x} \ln\left(1 + \frac{R_{Ox}^{CO_x}}{\exp\left(-\frac{t_{OH}}{\lambda_{OH}}\right) \exp\left(-\frac{t_{SurfO}}{\lambda_{SurfO}}\right)}\right) \quad (8)$$

$$t_{H_2O} = \lambda_{H_2O} \ln\left(1 + \frac{R_{Ox}^{H_2O}}{\exp\left(-\frac{t_{OH}}{\lambda_{OH}}\right) \exp\left(-\frac{t_{SurfO}}{\lambda_{SurfO}}\right) \exp\left(-\frac{t_{CO_x}}{\lambda_{CO_x}}\right)}\right) \quad (9)$$

where

$$R_j^i \equiv \frac{I_i}{I_j} \left( \frac{N_j \sigma_j \lambda_j}{N_i \sigma_i \lambda_i} \right) \quad (10)$$

The inelastic mean free path ( $\lambda$ ) was obtained from Gries inelastic scattering model and predictive equation<sup>1</sup> using the density of reference compounds (Table S2).

Peak name	Material	$\rho$ (gr cm-3)	$\lambda$ (nm) [1000 eV]	$\lambda$ (nm) [700 eV]	N (nm-3)
Water	H2O	0.997	2.43	1.4	33
Oxyde	SrTiO3	4.81	1.28	0.7	45
Hydroxyls	Ti(OH)4	3*	1.44	0.8	
	Sr(OH)2	3.62	1.58	0.9	50
COx**	H2CO3	1.67	1.87	1	
	SrCO3	3.5	1.6	0.9	47
SurfO***	SrTiO3	4.81	1.28	0.7	45

**Table S2:** Densities, calculated  $\lambda$  and atomic densities (N). \* estimated from densities of hydroxides. \*\*Values for Titanium carbonate not found. \*\*\* Same values as STO were used. When two  $\lambda$  are provided, a mean value of the two  $\lambda$  was used.

A monolayer coverage (ML) of the different species are defined as a given thickness for each species as already used in similar models in the literature:<sup>2</sup>  $ML_{\text{water}} = 0.31$  nm,  $ML_{\text{Hydroxyls}} = 0.31$  nm,  $ML_{\text{COx}} = 0.45$  nm,  $ML_{\text{SurfO}} = 0.39$  nm. Definition of ML for each species is an approximation based on the the molecular size or the crystal structure of the different materials considered in Table S2. Definition of water monolayer is based in average thickness of a molecular layer in bulk water at 298 K. It's clear that water monolayer in contact with the surface can have different

structures and densities and this thickness has to be taken as an approximation or a comparison with bulk water.

The two main parameters that affect ML calculation in the model are  $N$  and  $\lambda$ . In figure S2 calculation of Hydroxyl ML is plotted for different spectra taken at different conditions (simply layer as a number from 1 to 15 ) for 700 eV of photon energy. The plot compares calculations for three different  $\lambda$  :  $\lambda = 0.7$ ,  $\lambda = 0.9$  and  $\lambda = 1.1$  (Figure S2a), three different  $N$ :  $N=40$ ,  $N=45$ ,  $N=50$  (Figure S2b) and comparing the maximum and minimum values by crossing the possible variations among  $\lambda$  and  $N$  (Figure S2c). Those calculations contribute to the estimated error included in Figure 3a and Figure 5c.

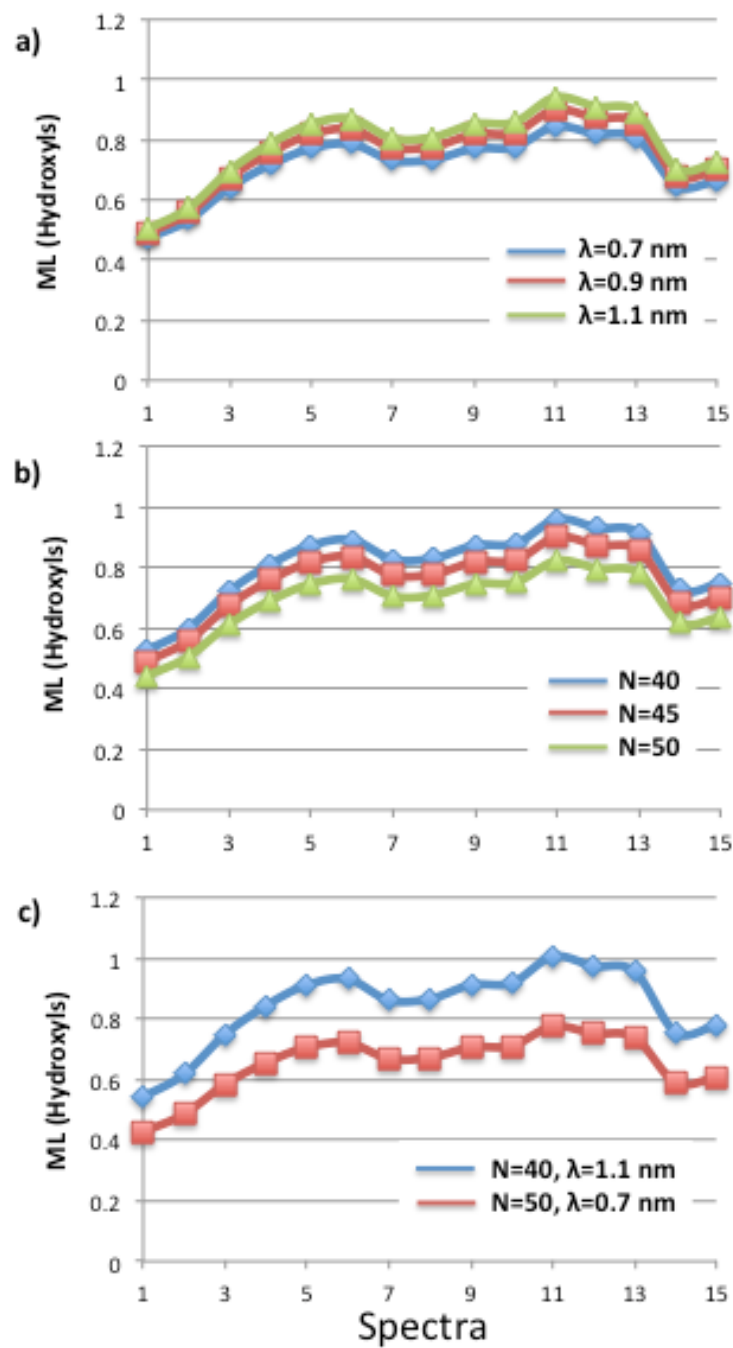


**Fig. S4:** ML Hydroxyls calculation for different spectra label 1 to 15 at different conditions as a function of the parameters  $\lambda$  and N.

## B4. Calculation for depth profile graph.

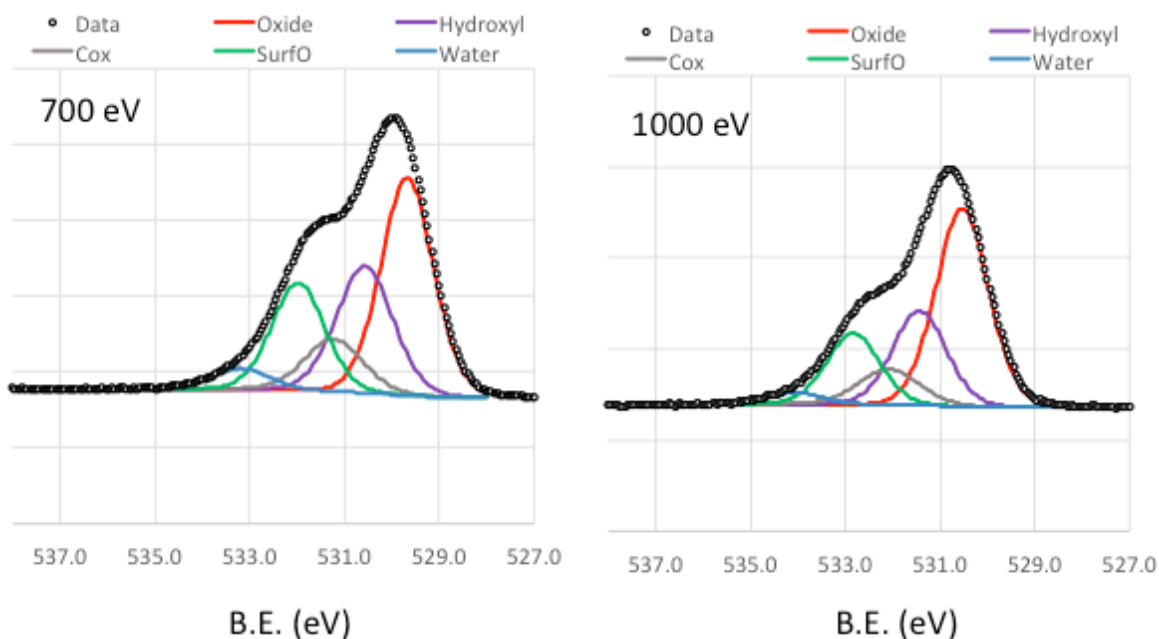


**Fig. S5:** O1s spectra measured at 700 eV and 1000 eV on the same spot at residual water vapour gas conditions (pressure < 10<sup>-3</sup> mbar) after the pressure and temperature experiments.

In order to visualize the relative differences among the two spectra and quantify the changes in the strength of the signal as a function of the depth of the out coming electrons (i.e., closer to the surface for the spectra measured with 700 eV and deeper in the bulk for the one at 1000 eV), as shown in Figure 2b, we performed the following calculation:

- a) We normalized the two spectra so that the oxide peak is equal for both, assuming that the signal of the oxide contribution should not be energy-(depth-)dependent, but equal for both of them.

$$Y_{oxide} = k \cdot XPS_{oxide\ 700} = k' \cdot XPS_{oxide\ 1000} = 1$$

- b) We took the intensities for each peak and compared them to the total intensity of the sum of the peak for the two spectra together:

$$Y_{i700} = \frac{k \cdot XPS_{i700}}{k \cdot XPS_{i700} + k' \cdot XPS_{i900}}$$

$$Y_{i900} = \frac{k' \cdot XPS_{i900}}{k \cdot XPS_{i700} + k' \cdot XPS_{i900}}$$

In this manner, the plotted value is a relative or percentage variation of the specie contribution with respect to an averaged value as a function of the depth of the out-coming electrons. Even it cannot be taken as an absolute value, it gives clear evidence of which specie has a more superficial/bulk contribution as compared to the others.

### C. Thickness of the adsorbates layer as a function of the pressure

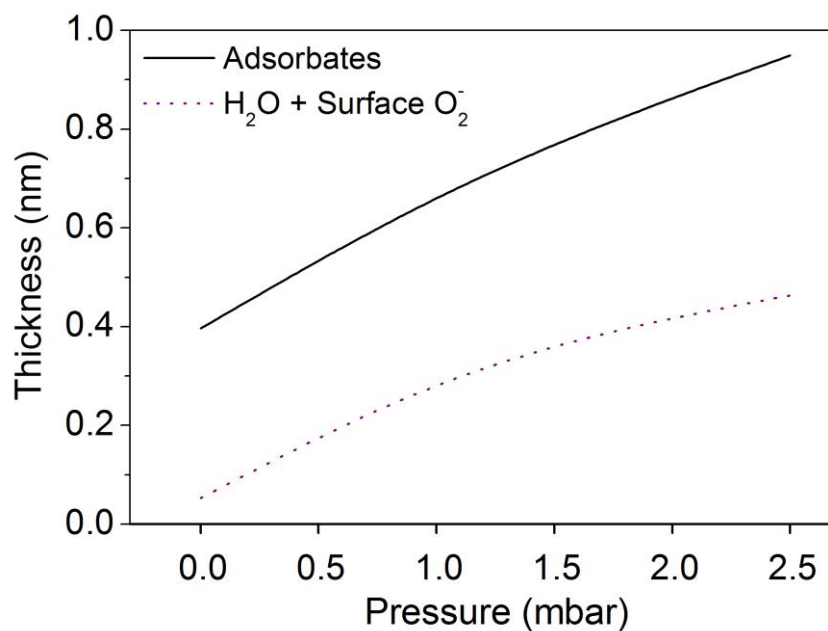


**Fig. S6:** Evolution of the total thickness of the adsorbates considered in the multilayer model ( $t_{\text{OH}}+t_{\text{CO}_x}+t_{\text{SurfO}}+t_{\text{water}}$ ) as a function of water vapor pressure (solid line), together with the thickness of the partial layer of adsorbates including only the contribution of water and peroxide species (dotted line).

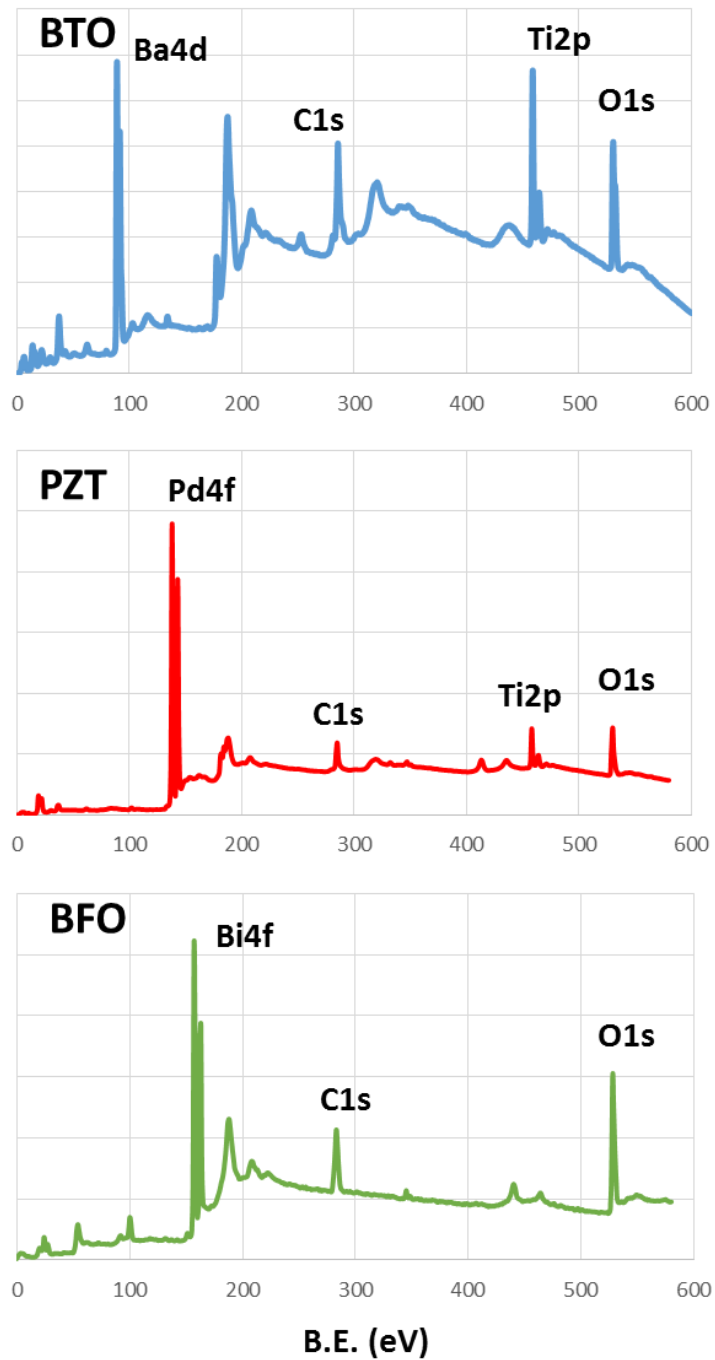


**Fig. S7:** Survey spectra of the three different ferroelectric perovskites mentioned in the manuscript measured at 700 eV

References:

- (1) Gries, W. H. A Universal Predictive Equation for the Inelastic Mean Free Pathlengths of X-ray Photoelectrons and Auger Electrons. *Surf. Interface Anal.* **1996**, 24, 38-50.
- (2) Stoerzinger, K. A.; Hong, W. T.; Crumlin, E. J.; Bluhm, H.; Biegalski, M. D.; Shao-Horn, Y. Water Reactivity on the LaCoO<sub>3</sub> (001) Surface: An Ambient Pressure X-ray Photoelectron Spectroscopy Study. *J. Phys. Chem. C* **2014**, 118, 19733–19741.